

Conditions for electron capture by an ultraintense stationary laser beam

Q. Kong,¹ Y. K. Ho,^{2,1,*} J. X. Wang,¹ P. X. Wang,¹ L. Feng,¹ and Z. S. Yuan¹

¹*Institute of Modern Physics, Fudan University, Shanghai 200433, China*

²*CCAST (World Laboratory), P. O. Box 8730, Beijing 100080, China*

(Received 1 July 1999)

We present in this paper a quantitative study of an effect, in which a low-energy free electron is captured and violently accelerated to GeV final kinetic energy by a stationary extra-high-intensity laser beam ($Q_0 \equiv eE/m_e\omega c \geq 100$). The conditions under which this phenomenon can occur, such as the momentum range, incident angle of the incoming electron, the waist width of the laser beam, etc., have been investigated in detail.

PACS number(s): 41.75.-i, 42.50.Vk

I. INTRODUCTION

As a result of the invention of the chirped pulse amplification (CPA) technique [1,2], laser intensities of 10^{20} W/cm² can now be achieved, and it is anticipated that intensities of 10^{22} W/cm² or higher will be reached in the near future [3]. For such lasers with 1 μ m wavelength, the electric field can be as high as 10^4 – 10^5 MV/cm, much larger than that of conventional accelerators, which is about 1–10 MV/cm magnitude. Thus, ever since the 1980s, there has been much research concerning how to make use of intense laser fields to accelerate particles, especially electrons, such as laser-induced beat-wave or wake-field electron accelerations by plasmas and inverse Cherenkov accelerations. But when media are involved, the difficulties of controlling medium breakdown and instabilities related to plasma-matter interactions cannot be solved easily. Hence, in our work, we will put the focus upon the electron acceleration by intense lasers in vacuum.

We have found in our previous study [4] that an electron can be accelerated to MeV energies when the laser intensity is large enough ($Q_0 \equiv eE_0/m_e\omega c \geq 10$, where Q_0 is a dimensionless parameter measure of the field intensity, $-e$ and m_e the electron's charge and rest mass, respectively, ω the laser circular frequency, and c the speed of light in vacuum). But MeV kinetic energy is too low for a practical accelerator because it is far less than what can be obtained with the present facilities, e.g., GeV electrons at SLAC. Recently we reported a phenomenon [5] that showed that an electron can be captured and violently accelerated to GeV energy by a laser beam with $Q_0 \geq 100$ (for a Nd:glass laser, this corresponds to a laser intensity of about 10^{22} W/cm²). This electron capture effect should be an effective mechanism of acceleration by lasers. However, this mechanism depends on many parameters, such as the electron's incident momentum and angle, the width of the laser beam, etc. For the purpose of practical application of such mechanism, it is necessary to probe the relationships between the capture effect with these

physics quantities, which is the main concern of this paper.

In the following, we will first present the numerical simulation model of the electron-laser interaction. Then attention is turned to the electron capture conditions. The conclusion is drawn in the last section.

II. CALCULATION MODEL

In our calculation, we adopt the field of lowest-order Hermite-Gaussian mode, which is x polarized and propagating along the z axis. The expression for the transverse electric component can be written as [6]

$$E_x = E_0 \frac{w_0}{w(z)} \exp\left(-\frac{x^2 + y^2}{w^2(z)}\right) \exp\left[i\left(\omega t - kz - \varphi(z) - \varphi_0 - \frac{k(x^2 + y^2)}{2R(z)}\right)\right], \quad (1)$$

where E_0 is the reference electric-field strength, w_0 is the beam width at the focus center, k the laser wave number, φ_0 the initial phase, and

$$w(z) = w_0 \left[1 + \left(\frac{2z}{kw_0^2}\right)^2\right]^{1/2}, \quad (2)$$

$$R(z) = z \left[1 + \left(\frac{kw_0^2}{2z}\right)^2\right], \quad (3)$$

$$\varphi(z) = \tan^{-1}\left(\frac{kw_0^2}{2z}\right). \quad (4)$$

The other electric and magnetic components can be obtained by using [7]

$$E_x = (i/k)(\partial E_x / \partial x), \quad (5)$$

$$\mathbf{B} = -(i/w)\nabla \times \mathbf{E}. \quad (6)$$

Figure 1 shows the configuration of the laser-electron interaction. To obtain the electron dynamics, the relativistic Lorentz equation

*Author to whom correspondence should be addressed. Address correspondence to Institute of Modern Physics, Fudan University, Shanghai 200433, China. Fax: +86-21-65104949. Electronic address: hoyk@fudan.ac.cn

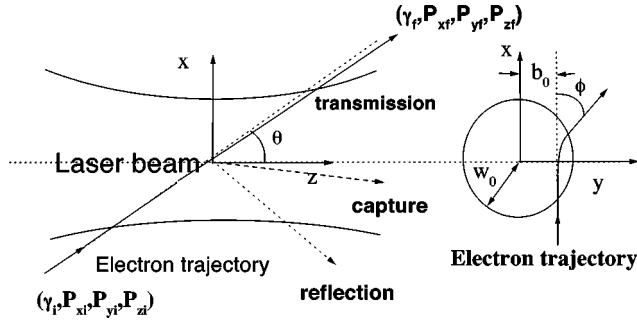


FIG. 1. Schematic geometry of electron scattering by laser beam. The laser propagates along the z axis. w_0 is the beamwidth at waist. Without losing generality, we assume electrons come in from the minus- x side parallel to the x - z plane. $(\gamma_i, P_{xi}, P_{yi}=0, P_{zi})$ denote the incoming energy and momentum of the electron and $(\gamma_f, P_{xf}, P_{yf}, P_{zf})$ that of the outgoing state. γ is the Lorentz factor and b_0 is the impact parameter. $\theta = \tan^{-1}(P_{xi}/P_{yi})$ is the electron incident angle, and $\phi = \tan^{-1}(P_{yf}/P_{xf})$ the deflection angle in the x - y plane.

$$\frac{d\mathbf{P}}{dt} = -e(\mathbf{E} + \mathbf{V} \times \mathbf{B}) \quad (7)$$

is solved numerically with the fourth-order Runge-Kutta method together with the Richardson's first-order extrapolation procedure [8], where V is the electron velocity in units of c . For simplicity, throughout this paper, length is normalized by $1/k$, time by $1/\omega$, and energy and momentum are normalized by $m_e c^2$ and $m_e c$, respectively.

III. RESULTS AND DISCUSSION

Previously the ponderomotive potential model [9,10] was widely used to analyze the free-electron motion in a laser field. By this model, the potential corresponding to a stationary laser beam of monofrequency is conservative, and electron scattering by this potential is bound to be elastic. This model stands well when the laser intensity is small. With the progresses in theory and experiment [4], when $Q_0 > 0.1$, the electron may be scattered inelastically by the intense laser beam. Moreover, when $Q_0 \geq 100$, incident electrons with low energy and small crossing angle relative to the laser propagation direction may not be reflected as predicted by the ponderomotive potential model. Instead, they will enter the strong-field region of the laser beam and keep moving along for a very long time as if captured by the laser beam. When this phenomenon happens, electrons can have net energy gain as high as 1 GeV. The ponderomotive model is totally invalid in describing this effect [5].

Previously three basic conditions under which the electron capture phenomenon may emerge had been determined. They are extra-high intensity, small crossing angle, and small transverse momentum P_{xi} relative to the extra-high intensity. The electron transverse momentum is a sensitive factor of the electron capture phenomenon. It should be much smaller than $Q_0/\sqrt{2}$. The value of $Q_0/\sqrt{2}$ was used in the ponderomotive model as a criterion for the reflection or penetration of an incident electron [4]. Of course, the electron incident momentum must not be too small, or else the

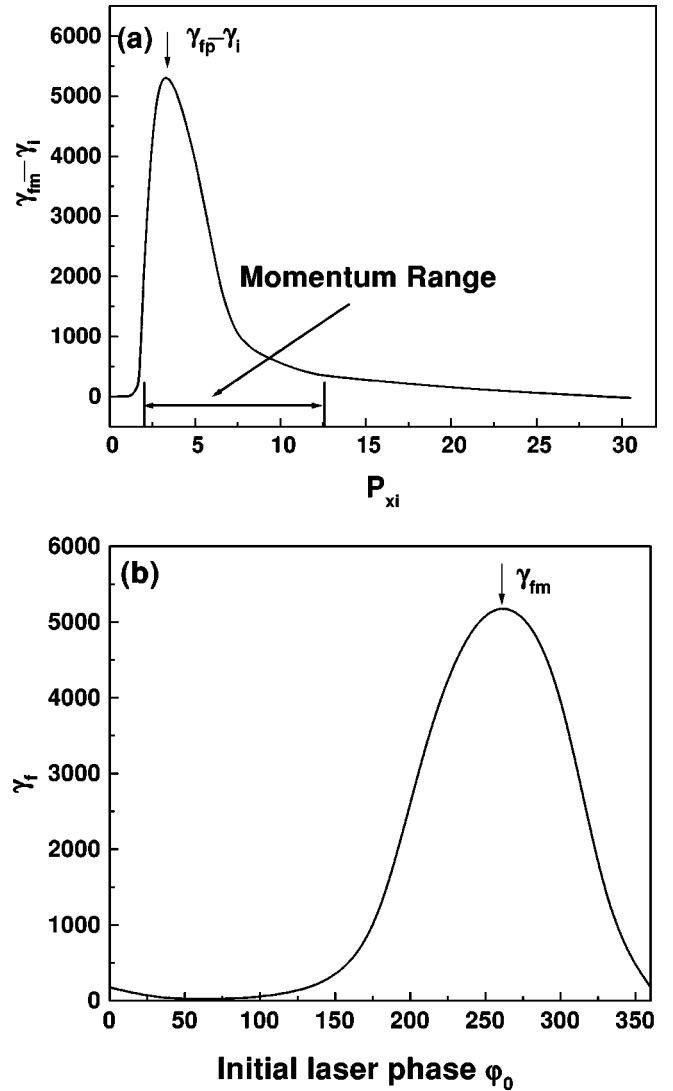


FIG. 2. (a) gives the maximum net electron energy gain, $\gamma_{fm} - \gamma_i$, as a function of the incident electron momentum P_{xi} . Through this paper, electron energy and momentum are measured in units of $m_e c^2$ and $m_e c$, respectively, length in the unit of $1/k$, and time in $1/\omega$. A laser beam of Hermite-Gaussian (0,0) mode with field intensity $Q_0 = 100$ and beamwidth $w_0 = 200$ is used. The electron comes in with $\theta = \tan^{-1}0.1$. The momentum range for the electron capture to occur is defined by the condition $\gamma_{fm} - \gamma_i > 300$. For a given P_{xi} (and so γ_i), the electron final energy γ_f is sensitive to the laser initial phase φ_0 [see Eq. (1)]. (b) presents a demonstration of the γ_f as a function of φ_0 for $P_{xi} = 3.5$, and from this figure one can get the corresponding value of the maximum final energy $\gamma_{fm} \sim 5200$. For capture cases, the calculation was terminated at $\omega t = 400\,000$.

electron cannot enter the strong-field region of the laser beam.

Figure 2(a) presents the variation of the maximum net electron energy gain, $\gamma_{fm} - \gamma_i$, with the incident electron momentum P_{xi} for a laser beam of a the Hermite-Gaussian (0, 0) mode with laser intensity $Q_0 = 100$, beamwidth $w_0 = 200$, and electron incident angle $\theta = \tan^{-1}0.1$. Here γ_{fm} is the maximum electron final energy. We note that when the values of the parameters Q_0 , w_0 , θ , and P_{xi} are given, the electron final energy γ_f is also strongly dependent on the

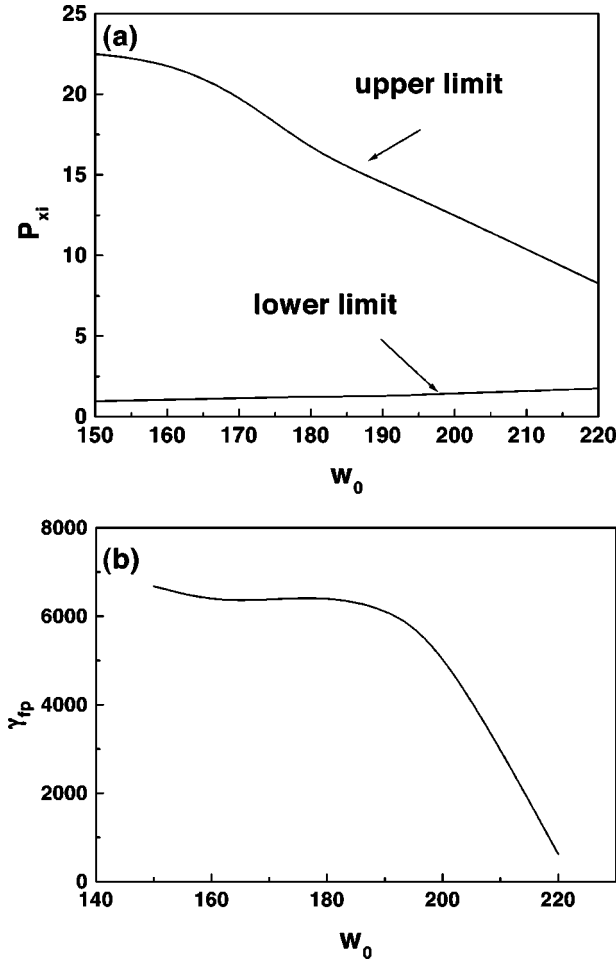


FIG. 3. Dependence of the momentum range for electron capture (a) and the dependence of the peak final electron energy γ_{fp} (b) on the beamwidth w_0 are shown. The laser beam and the electron incident angle are the same as those in Fig. 2 but the beamwidth varies. In (a), the top curve represents the capture momentum upper limit and the bottom curve for the lower limit. The momentum range for electron capture is between these two curves. To understand the way to get the curves in Fig. 3, Fig. 2(a) can be regarded as an example from which one may specifically extract the values of the momentum range and γ_{fp} for laser beamwidth $w_0 = 200$.

laser initial phase φ_0 [see Eq. (1)]. Figure 2(b) gives an example showing γ_f as a function of φ_0 for $P_{xi} = 3.5$ with other parameters being the same as in Fig. 2(a). From Fig. 2(b) one can extract the value of γ_{fm} for $P_{xi} = 3.5$. If we define the electron capture phenomenon to occur by the condition $\gamma_{fm} - \gamma_i > 300$, then from Fig. 2(a) one can see that the minimum incident momentum P_{xi} for the electron capture phenomenon to occur is near $P_{xi} = 1.5$. For $P_{xi} > 1.5$, γ_{fm} kept increasing and reached 1 GeV near $P_{xi} = 2.0$. When P_{xi} increased to near 3.2, the electron net energy gain reached its peak value $\gamma_{fm} - \gamma_i \sim 5400$, corresponding to the peak final energy of about $\gamma_{fp} \sim 2.7$ GeV. After that, γ_{fm} kept decreasing with increasing incident momentum until the electron capture phenomenon disappears when $P_{xi} > 12.5$. Thus one gets that the momentum range for electron capture to occur is $1.5 < P_{xi} < 12.5$ under the given conditions. Correspondingly, the incident electron energy ranges $7.7 \text{ MeV} < \gamma_i < 64 \text{ MeV}$. In the range $2.0 < P_{xi} < 6.0$, corresponding to the

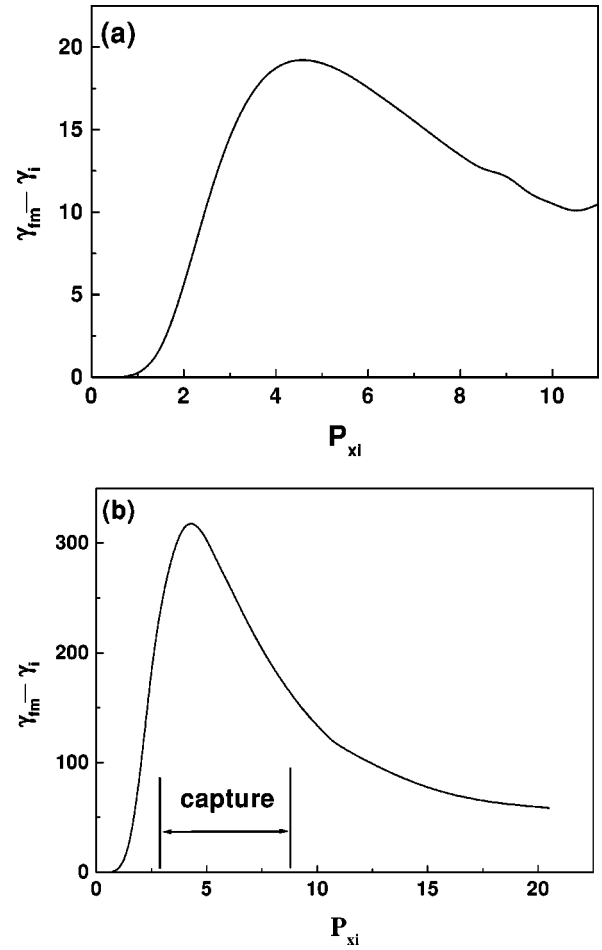


FIG. 4. The same as in Fig. 2(a) but for electron incident angle $\theta = \tan^{-1} 0.15$ and laser beamwidth $w_0 = 200$ (a), as well as $w_0 = 150$ (b).

electron incident energy being around 10–30 MeV, the incident electron can get up to GeV energy from the laser beam. From the results listed above, we can say more specifically that the electron must have incident energy in the range of 10–30 MeV, in order to get violently accelerated. This should be one advantage of this acceleration scheme, since it does not need to preaccelerate the electron to a high energy.

We go on to discuss now the influence of the beamwidth at the focus center w_0 on the momentum range in which the electron capture occurs. The results presented in Fig. 3(a) show that this momentum range depends sensitively on the beamwidth. In this figure, the top curve shows the maximum momentum and the bottom curve the minimum momentum where the electron capture can occur. One can see that as w_0 decreases, the lower limit of this momentum range decreases slightly. When $w_0 = 220$, this value is about 2.00, and when $w_0 = 150$, it is about 0.95. On the other hand, the upper limit of this momentum range keeps increasing substantially along with decreasing w_0 . When $w_0 = 220$, the momentum range for the capture effect is $[2.00, 8.25]$, while $[0.95, 22.5]$ for $w_0 = 150$. Thus, the range of incident momentum within which the electron capture occurs varies inversely with the beamwidth. We found also that the peak electron final energy γ_{fp} [see Fig. 2(a) for its definition] is influenced by the beamwidth. As shown in Fig. 3(b), when $w_0 = 150$, γ_{fp} reaches 6680, corresponding to 3.4 GeV, and then γ_{fp} varies

slightly with increasing w_0 . When $w_0 > 190$, it goes down quickly.

In our previous investigations [4,11] of electron scattering by a laser beam, the electron incident angle θ relative to laser beam's propagation direction was an important parameter. Only when θ is small enough ($\theta \ll \pi/4$) would the electron scattering proceed inelastically. Hence, it is no wonder that the electron capture is also sensitive to the incident angle. If the angle changes a little, the capture conditions will change a lot. All the discussion above is based on $\theta = \tan^{-1}0.1$. When we change the electron crossing angle to $\theta = \tan^{-1}0.15$, as shown in Fig. 4, electron capture does not occur at all when $w_0 = 200$ [Fig. 4(a)], because all the electrons are scattered by the laser beam soon after they incident on the laser beam and the maximum net energy gain is only tens of MeV. At $w_0 = 150$ [Fig. 4(b)], in some cases, electrons can be captured by the laser beam when $\gamma_{fm} - \gamma_i$ increases to a few hundred MeV, and in that case we may say that the electron is weakly captured.

IV. CONCLUSIONS

In summary, we have discussed in detail the conditions under which relatively low-energy electrons can be captured

by a ultraintense stationary laser beam. We present here the momentum ranges for electron capture under different laser beamwidths and the maximum energy and electron gains from the laser beam in each case. Based on our numerical analysis, the momentum range for electron capture becomes narrow with increasing beamwidth. We also presented the influence of the electron incident angle. All these findings may hopefully help the development of far-field electron accelerators based on the electron capture effect.

There are many questions left open to further discussion, such as the quantum physics underlying the complex electron capture phenomenon, the wave damping caused by the multielectron bunches accelerated by the wave, etc. We do plan to study those questions in the future.

ACKNOWLEDGMENTS

The authors would like to thank Professor C. M. Fou for carefully reading this manuscript and enlightening discussions. This work is partly supported by the National Natural Science Foundation of China under Contract No. 19684001, the National High-Tech ICP Committee in China, and the Science and Technology Funds of CAEP.

-
- [1] D. Strickland and G. Mourou, *Opt. Commun.* **264**, 219 (1985).
 - [2] P. Maine, D. Strickland, M. Pessot, and G. Mourou, *IEEE J. Quantum Electron.* **24**, 298 (1988).
 - [3] M.D. Perry and G. Mourou, *Science* **264**, 917 (1994).
 - [4] Y.K. Ho, J.X. Wang, L. Feng, W. Scheid, and H. Hora, *Phys. Lett. A* **220**, 189 (1996); J.X. Wang, Y.K. Ho, W. Scheid, and H. Hora, *ibid.* **231**, 139 (1997).
 - [5] J.X. Wang, Y.K. Ho, Q. Kong, L.J. Zhu, L. Feng, S. Scheid, and H. Hora, *Phys. Rev. E* **58**, 6575 (1998); L.J. Zhu, Y.K. Ho, J.X. Wang, and Q. Kong, *Phys. Lett. A* **248**, 319 (1998).
 - [6] Orazio Svelto and David C. Hanna, *Principles of Lasers*, 3rd ed. (Plenum Press, New York, 1989).
 - [7] Melvin Lax, *Phys. Rev. A* **11**, 1365 (1975); L.W. Davis, *ibid.* **19**, 1177 (1979).
 - [8] M.L. James, G.M. Smith, and J.C. Wolford, *Applied Numerical Method for Digital Computation*, 3rd ed. (Harper and Row, New York, 1985).
 - [9] F. Martin *et al.*, in *Advanced Acceleration Concepts*, edited by F.E. Mills, AIP Conf. Proc. No. 156 (AIP, New York, 1981).
 - [10] T.W. Kibble, *Phys. Rev.* **138**, B740 (1965).
 - [11] J.X. Wang, Y.K. Ho, and W. Scheid, *Phys. Lett. A* **234**, 415 (1997).